

Vibrationally resolved partial cross sections and asymmetry parameters for carbon K-shell photoionization of the CO₂ molecule

M Hoshino¹, K Nakagawa¹, T Tanaka¹, M Kitajima^{1,6}, H Tanaka¹,
A De Fanis^{2,7}, K Wang³, B Zimmermann^{3,4,8}, V McKoy³ and K Ueda⁵

¹ Department of Physics, Sophia University, Tokyo 102-8554, Japan

² Japan Synchrotron Radiation Research Institute, Sayo-gun, Hyogo 679-5198, Japan

³ AA Noyes Laboratory of Chemical Physics, California Institute of Technology, Pasadena, CA 91125, USA

⁴ Max-Planck Institute for the Physics of Complex Systems, 01187 Dresden, Germany

⁵ Institute of Multidisciplinary Research for Advanced Materials, Tohoku University, Sendai 980-8577, Japan

E-mail: masami-h@sophia.ac.jp and ueda@tagen.tohoku.ac.jp.

Received 10 April 2006, in final form 23 May 2006

Published 11 July 2006

Online at stacks.iop.org/JPhysB/39/3047

Abstract

We have measured the vibrationally resolved partial cross sections $\sigma_{v'_1}$ and asymmetry parameters $\beta_{v'_1}$ for C K-shell photoionization of the CO₂ molecule in the Σ_u shape resonance region above the C K-shell ionization threshold. The positions of both the maxima of $\sigma_{v'_1}$ and the minima of $\beta_{v'_1}$ move towards the C K-shell threshold with increasing symmetric stretching vibrational excitation v'_1 in the C 1s single-hole state. Calculations employing the relaxed-core Hartree–Fock approach reproduce the observed vibrational effects.

(Some figures in this article are in colour only in the electronic version)

1. Introduction

An electronic transition in a molecule results in the redistribution of the electron density. As the nuclear conformation cannot adapt to this redistribution on the same time scale, the final state of the molecule is often vibrationally excited. This is also the case for molecular photoionization where photoemission is accompanied by vibrational excitation of the residual molecular ion. Recent high-resolution soft x-ray photoelectron spectroscopic studies [1–11] show that the spectral and angular distributions for inner-shell photoemission from molecules

⁶ Present address: Department of Chemistry, Tokyo Institute of Technology, Tokyo 152-8551, Japan.

⁷ Present address: Shimadzu Research Laboratory, Wharfside, Trafford Wharf Road, Manchester, M17 1GP, UK.

⁸ Present address: Department of Physics & Astronomy, Louisiana State University, Baton Rouge, LA 70803, USA.

in shape resonance regions depend on the final vibrational state, as predicted theoretically some decades ago [12, 13].

Among the best studied examples of this behaviour is the inner-shell photoionization of carbon monoxide, CO, where Bradshaw and co-workers [1, 3] found that the position of the individual vibrational components in the region of the Σ shape resonance in C 1s photoionization varies from ~ 307 eV for $v' = 0$ to ~ 302 eV for $v' = 3$. A shift in the opposite direction is observed for the Σ shape resonance in the O 1s photoionization spectra [6]. Mistrov *et al* [6] interpreted these downward and upward shifts of the Σ shape resonance to be a result of intramolecular interference of the scattered photoelectron waves in the CO molecule where the effective C–O distance, R , increases and decreases, respectively, with an increase in v' , for the C and O 1s single-hole states [6]. This interpretation is consistent with the results of elaborate theoretical calculations for the C and O K-shell photoionization cross section for different v' states, where R -dependent dipole amplitudes are averaged over R with the vibrational wavefunctions of the initial and final states [7, 14].

There have also been studies of the K-shell photoionization of nitrogen molecules N_2 [10] and of C K-shell photoionization of acetylene C_2H_2 [11]. Compared to CO, N_2 shows an additional complication. The N K-shell single-hole state splits into gerade and ungerade levels which are separated by only 100 meV, and the C K-shell single-hole state of C_2H_2 also splits into gerade and ungerade states with a separation of 100 meV. The C–C stretching vibration is seen predominantly in the C K-shell single-hole state. Measurements in both N_2 and C_2H_2 show a vibrational-state dependence of the partial cross sections $\sigma_{g,v'}$ and the asymmetry parameters $\beta_{g,v'}$, similar to C K-shell photoionization of CO. *Ab initio* calculations for N_2 employing the random phase approximation by Semenov *et al* [10] reproduced the vibrational dependence of $\sigma_{g,v'}$ and $\beta_{g,v'}$ quite well.

These studies [6, 7, 10, 11] illustrate the important role of nuclear dynamics in shape resonance phenomena and motivated us to extend these studies to a linear triatomic molecule CO_2 . The CO_2 molecule has four vibrational modes, the symmetric ($v'_1, 0, 0$) and anti-symmetric ($0, 0, v'_3$) stretching modes and a doubly degenerate bending mode ($0, v'_2, 0$), and one might thus expect vibrational excitation of these modes to accompany photoionization of CO_2 . It is known, however, that C 1s ionization is accompanied by excitation of the symmetric stretching vibrations ($v'_1, 0, 0$) [15], whereas O 1s ionization is accompanied by excitation of antisymmetric vibrations ($0, 0, v'_3$) [4, 15–17]. In previous theoretical studies of the Σ_u shape resonance in K-shell photoionization of CO_2 [18–20] effects of vibrational excitations were ignored.

In the present work, we report on results of experimental and theoretical studies of vibrational effects on the spectral dependence of the C K-shell photoionization cross sections $\sigma_{v'_1}$ and the asymmetry parameters $\beta_{v'_1}$ of CO_2 in the Σ_u shape resonance region.

2. Experiment

The experiments were carried out on the C branch of the soft x-ray photochemistry beam line 27SU [21, 22] at SPring-8, the 8 GeV synchrotron radiation facility in Japan. The radiation source is a figure-8 undulator providing radiation linearly polarized either in the horizontal plane of the storage ring (1st order) or in the vertical plane perpendicular to it (0.5th order) [23]. Angle-resolved electron emission measurements were performed only by changing the undulator gap and without rotation of the electron analyser. The electron spectroscopy apparatus consists of a hemispherical electron analyser (Gammadata–Scienta SES2002), a gas cell and a differentially pumped chamber [24].

The degree of linear polarization was determined by observing the Ne 2s and 2p photolines and confirmed to be greater than 0.98 with the present setting of the optics [25]. In the analysis we thus assume complete polarization at the photon energies employed. The photon flux was measured by a photocurrent on the refocusing mirror before the gas cell. In the C 1s ionization region, however, measurements of the photon flux by photocurrent suffer from carbon contamination on the surface of the optical components and the photon flux reading was thus corrected by comparing intensities of angle-resolved Ar 2p photoelectron spectra with the known cross sections and angular distributions at the photon energy of interest. The transmission of the electron analyser is not constant in the electron energy range of interest and was corrected by comparing the Ne 1s and Ar 2p photoelectron spectra with known cross sections and angular distributions. Each angle-resolved photoelectron spectrum was fitted, once these corrections were included.

3. Theory

The carbon K-shell photoionization cross sections and asymmetry parameters of CO₂ were calculated within a relaxed-core Hartree–Fock (RCHF) approximation in a molecular basis set obtained using Slater’s transition state approximation [26]. In this approximation the relaxed molecular orbitals are derived from a self-consistent field calculation where only half the charge of an electron is removed from the carbon K-shell. The procedure attempts to capture effects arising from the screening of the K-shell hole after ionization, while maintaining the calculation at the one-electron level. To avoid working with nonorthogonal orbitals, we also use this molecular basis to construct the initial N -electron state and the final N -electron state with an electron in the continuum [27]. Ionization out of this C K-shell orbital in the ground vibrational state results in a distribution of ion vibrational levels in the symmetric stretch mode. For linearly polarized light, the vibrationally resolved differential cross sections and asymmetry parameters can be expressed as

$$\frac{d\sigma_{v'_1}}{d\Omega} = \frac{\sigma_{v'_1}}{4\pi} [1 + \beta P_2(\cos \theta)], \quad (1)$$

where $\sigma_{v'_1}$ is the total cross section for the ion vibrational state v'_1 , β is the asymmetry parameter, θ is the angle between the polarization vector of the light and the momentum of the electron and $P_2(\cos \theta)$ is the Legendre polynomial of degree 2. The total photoionization cross section averaged over all polarization and photoelectron directions is given by

$$\sigma_{v'_1} = \frac{4\pi^2}{3c} E \sum_{\ell\lambda\mu} |I_{\ell\lambda\mu}^{v'_1}|^2, \quad (2)$$

where c is the speed of light, E is the photon energy, ℓ is a photoelectron partial wave, λ is the projection of its angular momentum on the molecular axis, μ is the photon index and $I_{\ell\lambda\mu}^{v'_1}$ is the vibrationally resolved dynamical coefficient. The vibrationally resolved dynamical coefficients are obtained by integration of the dynamical coefficients, $I_{\ell\lambda\mu}(R)$, over the vibrational wavefunctions of the neutral and ionic states. The vibrational wavefunctions are obtained assuming harmonic potentials for both the neutral and ion.

The R -dependent dynamical coefficients, $I_{\ell\lambda\mu}(R)$, are given by

$$I_{\ell\lambda\mu}(R) = (k)^{1/2} \langle \Psi_i | r_\mu | \Psi_{f,k\ell\lambda}^{(-)} \rangle \quad (3)$$

in the dipole length form, where k is the momentum of the photoelectron, Ψ_i is the ground-state wavefunction and $\Psi_{f,k\ell\lambda}^{(-)}$ is the incoming-wave normalized final state wavefunctions. The

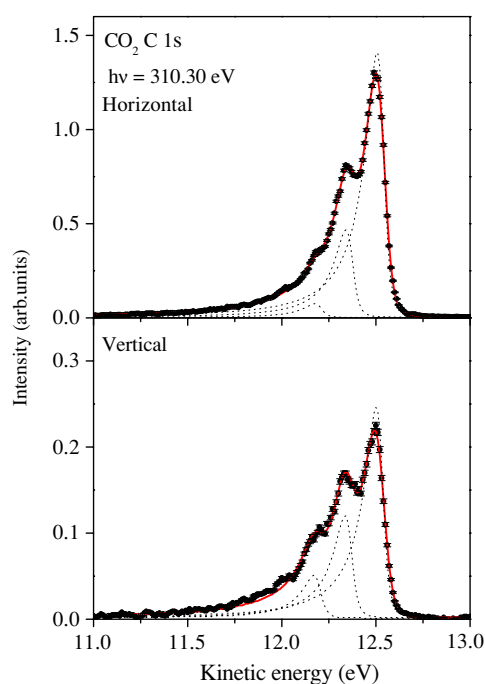


Figure 1. C K-shell photoelectron spectra of CO₂ at a photon energy of 310.30 eV. Upper and lower frames: parallel and perpendicular to the polarization vector, respectively. Open circles—experiment; thick solid lines—a least-squares fit; thin dashed lines—individual components of the fitting but without instrumental broadening.

photoelectron orbitals $\Psi_{f,k\ell\lambda}^{(-)}$ are obtained using an iterative procedure to solve the Lippmann–Schwinger equation associated with the one-electron Schrödinger equation [28] with a potential produced by the transition-state orbitals. Two iterations produced converged results in this study.

We employed the same basis set used in previous studies of CO [29] to obtain the HF wavefunction of the neutral molecule and used 19 internuclear distances between C and O ranging from 1.72 to 2.53 a_0 to obtain the vibrationally-averaged dynamical coefficients. The calculations were carried out in both length and velocity forms. The agreement between both sets of cross sections is excellent and only results from the length form are presented here.

4. Results and discussion

Figure 1 shows the C 1s photoelectron spectra of CO₂ measured at 0° and 90° relative to the polarization vector at a photon energy of $E = 310.3$ eV, i.e. 12.6 eV above the C 1s ionization threshold [30]. These spectra have been normalized for the photon flux and gas pressure and corrected for the transmission function. The error bars in figure 1 come from the statistical uncertainties based on the electron counts and are 0.75% and 1.8% for the horizontal and vertical spectra, respectively, at the peaks of the photoelectron spectra. The spectra exhibit one vibrational progression due to symmetric stretching ($\nu'_1, 0, 0$). Each partial cross section was determined from the intensity of the individual components in the angle-resolved spectra. The effect of post-collision interaction (PCI) was included by simulating the individual profiles with the equation of van der Straten [31]. The PCI profile was convoluted

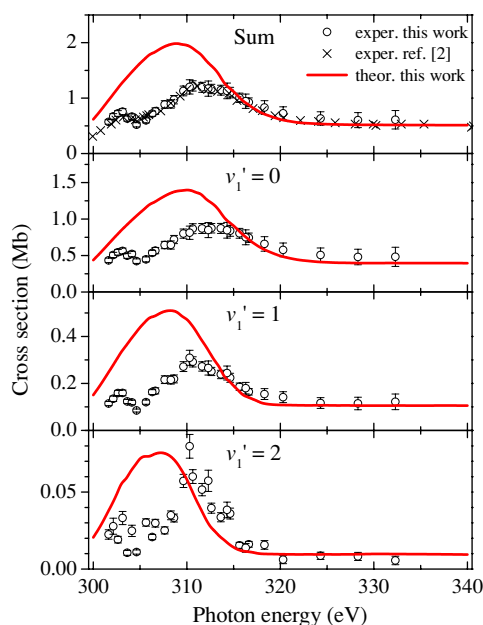


Figure 2. C K-shell single-hole photoionization cross sections $\sigma_{v_1'}$ of CO₂, for $v_1' = 0, 1, 2$ and their sum. Calculated results (red solid lines) in the RCHF approximation with a fractional charge of 0.5 are shown together with the experimental data (open circles: present results; crosses: Schmidbauer *et al* [2]).

with a Gaussian to account for instrumental broadening. We first performed the fitting to a few spectra whose signal-to-noise ratios were sufficiently good, treating the frequencies and Gaussian and Lorentzian widths, as well as intensities of the individual vibrational components as fitting parameters. The fitting yielded a Gaussian full-width-at-half-maximum (FWHM) value of 50(2) meV. This value is consistent with the total instrumental width estimated from the analyser bandwidth of 25 meV (slit width of 4 mm and pass energy of 2 eV), photon bandwidth of 40 meV and the Doppler broadening of 8.5 meV. The resulting natural width (FWHM) is 98(2) meV, in reasonable agreement with the natural widths 103(1), 100(1) and 99(2) meV at photon energies 308, 320 and 330 eV, respectively, reported by Carroll *et al* [32]. The fitting also gave a vibrational frequency of 165(1) meV, in reasonable agreement with 168(1), 164(1) and 166(1) meV at photon energies 308, 320 and 330 eV, respectively, as reported by Carroll *et al* [32]. We found that the $v_1' = 3$ cross section is less than 30% of the $v_1' = 2$ cross section, and that the $v_1' = 2$ cross section may be overestimated by 20% at most by neglecting the $v_1' = 3$ contribution. In the fitting of the whole data set, we fixed the natural lifetime width and vibrational spacing obtained above, while we treated the intensities of the individual lines and the Gaussian width as fitting parameters. We did not include the $v_1' \geq 3$ components in the fitting.

The spectral dependence of the measured C 1s single-hole photoionization cross sections $\sigma_{v_1'}$ for $v_1' = 0, 1, 2$ and their sum are shown in figure 2. The present vibrationally summed measurements (open circles) agree well with the previous vibrationally unresolved measurements (crosses) of Schmidbauer *et al* [2]. The absolute scale in figure 2 is based on the measurements of Schmidbauer *et al*; the present measurement only provides the relative scale and is thus normalized to the result of Schmidbauer *et al* at the resonance energy ~ 313 eV. The Σ_u shape resonance is clearly seen in the spectral dependence of $\sigma_{v_1'}$ as well as

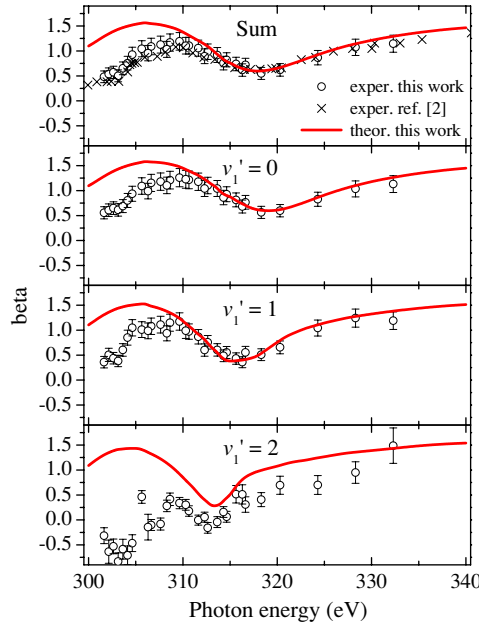


Figure 3. Photoelectron asymmetry parameters $\beta_{v'_1}$ for C K-shell single-hole photoionization of CO_2 , for $v'_1 = 0, 1, 2$ and the average of these v'_1 values. See caption of figure 2 for details.

in the vibrational sum σ_{CK} . The shape resonance appears at 313 eV for $\sigma_{v'_1=0}$ and moves slightly downwards to the C K-shell threshold with increasing v'_1 . This v'_1 dependence of the shape resonance energy is similar, though less pronounced, to the case of the Σ shape resonance in C K-shell photoionization of CO [1, 3, 6]. The second small peak around 303 eV in all three spectra is due to a doubly-excited autoionizing state. In the present calculations, these doubly excited states are not taken into account. The spectral dependence of the calculated $\sigma_{v'_1}$ for $v'_1 = 0, 1, 2$ and σ_{CK} is also shown in figure 2 where the calculated σ_{CK} are seen to agree well with the measured (absolute) values at energies well above the shape resonance. Below the shape resonance the agreement between the calculated and measured cross sections is much less satisfactory. We attribute the difference to the presence of autoionizing resonances in this region, which are not included in our description of the photoionization process. The Hartree–Fock description employed here provides only the smooth continuum background of the photoelectron wavefunction and does not account for the coupling of resonance-like structures with this background. Moreover, though the length and velocity forms of the present cross sections are quite close, the cross sections provided by this model do not satisfy any sum rules. The calculated $\sigma_{v'_1}$ also reproduce the intensity ratios for different v'_1 quite well. Furthermore, the calculated positions of the shape resonance shift downwards with increasing v'_1 , though the downward shift is larger than observed.

Figure 3 shows the measured asymmetry parameters $\beta_{v'_1}$ for $v_1 = 0, 1, 2$ and $\beta_{\text{CK}} \equiv \sum_{v'_1} \beta_{v'_1} \times \sigma_{v'_1} / \sigma_{\text{CK}}$ as a function of photon energy. The energy dependence of the measured β_{CK} (open circles) agrees well with the previous measurements of Schmidbauer *et al* [2]. The Σ_u shape resonance is responsible for the characteristic photon energy dependence of $\beta_{v'_1}$: a maximum below and a minimum above the shape resonance and a dispersive-type profile. The dip in $\beta_{v'_1}$ appears at 319 eV for $\beta_{v'_1=0}$, and moves towards threshold with increasing v'_1 , while the dip deepens with increasing v'_1 . The calculated $\beta_{v'_1}$ and β_{CK} are also shown in

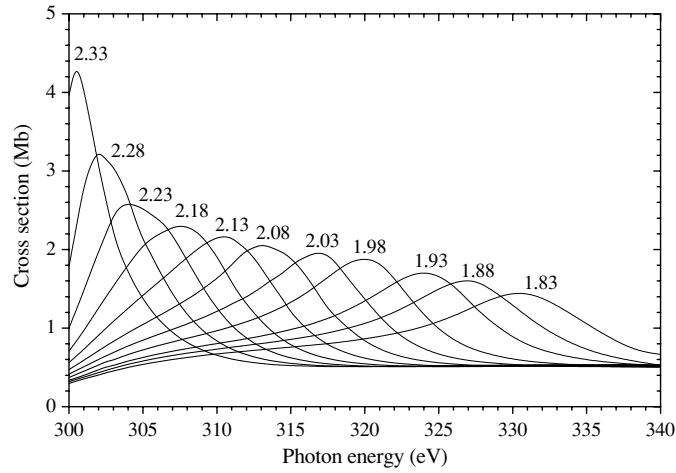


Figure 4. C K-shell single-hole photoionization cross sections $\sigma_{R_{C-O}}$ of CO₂ for fixed C–O distances of R_{C-O} (a_0) given in the figure.

figure 3, where they are seen to reproduce the measurements above 310 eV quite well, including the dip in β_{CK} observed at 316 eV. The calculated $\beta_{v'_1}$ also show the observed behaviour of the dip which moves down in energy and deepens with increasing v'_1 . The agreement is poorer for $v'_1 = 2$. This may be due to the contribution from $v'_1 = 3$, which was excluded in the present fitting. Below 310 eV, the agreement between the measurements and the calculations becomes poorer with decreasing energy, e.g., the additional dip structure below 305 eV. This structure can be attributed to the doubly-excited autoionizing states, which are not taken into account in the present calculations.

Following Dehmer and co-workers [12, 13], we can explain the origin of the v'_1 dependence of the peak energy in the cross section σ and the dip in the asymmetry parameter β as follows. The shape resonance arises from trapping of the photoelectron by a potential barrier. This barrier, and hence the energy and width of the resonance, is a sensitive function of the C–O distance (R_{C-O}) and varies significantly over the range of R_{C-O} corresponding to the ground-state zero-point vibrational motion. Figures 4 and 5 show $\sigma_{R_{C-O}}(E)$ and $\beta_{R_{C-O}}(E)$ as a function of photon energy for C–O distances in the range $1.83a_0$ and $2.33a_0$. The equilibrium C–O distance in the neutral ground state is $2.196a_0$ and $2.16a_0$ in the C 1s ionized state. In these figures, the shape resonance is seen to shift to lower kinetic energy and to become narrower and more strongly peaked as R_{C-O} increases while the dip in the asymmetry parameter shifts to lower kinetic energy as R_{C-O} increases. This behaviour reflects the sensitivity of the resonance to R_{C-O} . The net transition moment for a particular vibrational channel, on the other hand, can be estimated as an average of the R_{C-O} -dependent dipole amplitude, weighted by the product of the initial and final state vibrational wavefunctions at each R_{C-O} . The v'_1 dependence of the shape resonance energy and the position of the dip in the β curve arise because transitions to alternative final vibrational states preferentially sample different regions of R_{C-O} . In particular, $v'_1 = 1, 2$ sample successively larger R_{C-O} on average than $v'_1 = 0$, causing the resonance in those vibrational channels to peak at lower energy than $v'_1 = 0$.

To clarify the above point we consider a Taylor expansion of the R -dependent dynamical coefficient $I_{\ell\lambda\mu}(R)$:

$$I_{\ell\lambda\mu}(R) \approx I_{\ell\lambda\mu}(R_e) + Q \left. \frac{dI_{\ell\lambda\mu}(R)}{dR} \right|_{R=R_e}, \quad (4)$$

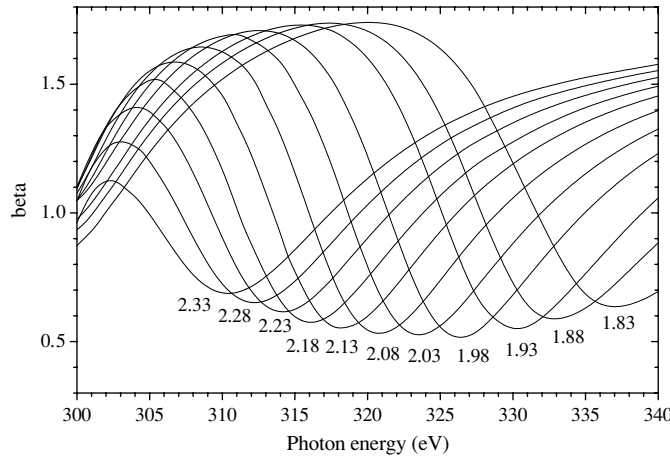


Figure 5. Photoelectron asymmetry parameters $\beta_{R_{C-O}}$ for C K-shell single-hole photoionization of CO₂ for fixed C–O distances of R_{C-O} (a_0) given in the figure.

where $Q = R - R_e$ and R_e is the equilibrium C–O distance in the neutral ground state. The vibrationally resolved dynamical coefficient $I_{\ell\lambda\mu}^{v'_1}$ is then given by

$$\begin{aligned} \langle 0 | I_{\ell\lambda\mu}(R) | v'_1 \rangle &\approx \langle 0 | v'_1 \rangle I_{\ell\lambda\mu}(R_e) + \langle 0 | Q | v'_1 \rangle \left. \frac{dI_{\ell\lambda\mu}(R)}{dR} \right|_{R=R_e} \\ &= \langle 0 | v'_1 \rangle I_{\ell\lambda\mu}(R_e + \Delta^{v'_1}), \end{aligned} \quad (5)$$

where

$$\Delta^{v'_1} = \frac{\langle 0 | Q | v'_1 \rangle}{\langle 0 | v'_1 \rangle} \quad (6)$$

is the effective displacement of the C–O distance for the individual v'_1 [6, 9]. We have calculated $\Delta^{v'_1}$ using equation (6) and found values of -0.0180 , 0.0514 and 0.1209 au for $v'_1 = 0, 1$ and 2 , respectively. The increase in $\Delta^{v'_1}$ with increasing v'_1 confirms the above qualitative discussion.

Finally, we briefly discuss the role of the nonspherical molecular potential on the photoionization dynamics. A single-centre expansion of the C 1s orbital about the carbon atom shows about 100% s-character at each internuclear distance. On the basis of atomic-like selection rules, a dominant p partial wave would be expected. However, in the shape resonance region around a kinetic energy of 10.5 eV, the partial-wave intensities are 0.183, 0.156, 0.053 and 0.003 au for p, f, h ($\ell = 5$) and j ($\ell = 7$), respectively, at $R_{C-O} = 2.18a_0$. The high intensity of the f partial wave is due to the shape resonance. Some interesting and unexpected behaviour can also be seen at higher kinetic energies. For example, at a kinetic energy of 42.5 eV (a photon energy of 340 eV), where the ratio of the cross sections for the ion vibrational states agrees well with Franck–Condon factors and the measured values, the partial wave contributions are 0.0301 (p), 0.0309 (f), 0.0313 (h ($\ell = 5$)) and 0.0100 (j ($\ell = 7$)) au, which are all quite comparable. This behaviour is strongly molecular and indicates that these partial waves arise from scattering of the photoelectron by the nonspherical molecular potential. The behaviour of the dynamical coefficients is similar for all internuclear distances.

5. Conclusions

We have reported on the results of measurements and calculations of the vibrationally resolved partial cross sections and asymmetry parameters for C K-shell photoionization of the CO₂ molecule in the symmetric stretching mode. Agreement between the calculated and measured spectral distributions of cross sections and asymmetry parameters is quite encouraging except in the region of shape resonance, where the calculations overestimate the effect of the shape resonance. The calculated positions of the shape-resonance peaks and the dips in the asymmetry parameters agree well with the measured values. The disagreement between the measurements and calculations at photon energies below the shape resonance may, at least in part, be attributed to the neglect of the doubly-excited autoionizing states in the calculations.

Acknowledgments

The experiment was carried out with the approval of the SPring-8 program review committee. This study was supported by Grants-in-Aid for Scientific Research from the Japanese Society for the Promotion of Science and a grant from the National Science Foundation (USA).

References

- [1] Randall K J, Kilcoyne A L D, Köppe H M, Feldhaus J, Bradshaw A M, Rubensson J-E, Eberhardt W, Xu Z, Johnson P D and Ma Y 1993 *Phys. Rev. Lett.* **71** 1156
- [2] Schmidbauer M, Kilcoyne A L D, Köppe H M, Feldhaus J and Bradshaw A M 1995 *Phys. Rev. A* **52** 2095
- [3] Köppe H M, Kempgens B, Kilcoyne A L D, Feldhaus J and Bradshaw A M 1996 *Chem. Phys. Lett.* **260** 223
- [4] Maier K, Kivimäki A, Kempgens B, Hergenbahn U, Neeb M, Rüdell A, Piancastelli M N and Bradshaw A M 1998 *Phys. Rev. A* **58** 3654
- [5] Piancastelli M N 1999 *J. Electron Spectrosc. Relat. Phenom.* **100** 167 and references therein
- [6] Mistrov D A, De Fanis A, Kitajima M, Hoshino M, Shindo H, Tanaka T, Tamenori Y, Tanaka H, Pavlychev A A and Ueda K 2003 *Phys. Rev. A* **68** 022508
- [7] Semenov S K, Cherepkov N A, De Fanis A, Tamenori Y, Kitajima M, Tanaka H and Ueda K 2004 *Phys. Rev. A* **70** 052504
- [8] Hergenbahn U 2004 *J. Phys. B: At. Mol. Opt. Phys.* **37** R89 and references therein
- [9] De Fanis A, Mistrov D A, Kitajima M, Hoshino M, Shindo H, Tanaka T, Tanaka H, Tamenori Y, Pavlychev A A and Ueda K 2005 *Phys. Rev. A* **71** 052510
- [10] Semenov S K *et al* 2006 *J. Phys. B: At. Mol. Opt. Phys.* **39** 375
- [11] Hoshino M *et al* 2006 *Chem. Phys. Lett.* **421** 256
- [12] Dehmer J L, Dill D and Wallace S 1979 *Phys. Rev. Lett.* **43** 1005
- [13] Dehmer J L, Dill D and Parr A C 1985 *Photophysics and Photochemistry in the Vacuum Ultraviolet* ed S McGlynn, G Findly and R Huebner (Dordrecht: Reidel) p 341
- [14] Semenov S K, Cherepkov N A, Jahnke T and Dörner R 2004 *J. Phys. B: At. Mol. Opt. Phys.* **37** 1331
- [15] Kivimäki A, Kempgens B, Maier K, Köppe H M, Piancastelli M N, Neeb M and Bradshaw A M 1997 *Phys. Rev. Lett.* **79** 998
- [16] Dobrodey N V, Köppel H and Cederbaum L S 1999 *Phys. Rev. A* **60** 1988
- [17] Saito N *et al* 2005a *Phys. Rev. A* **72** 042717
- [18] De Fanis A *et al* 2002 *Phys. Rev. Lett.* **89** 023006
- [19] Saito N *et al* 2003 *J. Phys. B: At. Mol. Opt. Phys.* **36** L25
- [20] Saito N *et al* 2005 *J. Phys. B: At. Mol. Opt. Phys.* **38** L277
- [21] Ohashi H, Ishiguro E, Tamenori Y, Kishimoto H, Tanaka M, Irie M, Tanaka T and Ishikawa T 2001 *Nucl. Instrum. Methods A* **467–68** 529
- [22] Ohashi H *et al* 2001 *Nucl. Instrum. Methods A* **467–68** 533
- [23] Tanaka T and Kitamura H 1996 *J. Synchrotron Radiat.* **3** 47
- [24] Shimizu Y *et al* 2001 *J. Electron Spectrosc. Relat. Phenom.* **114–116** 63
- [25] Yoshida H, Senba Y, Morita M, Goya T, De Fanis A, Saito N, Ueda K, Tamenori Y and Ohashi H 2004 *AIP Conf. Proc.* **705** 267

- [26] Slater J C 1974 *The Self-Consistent Field for Molecules and Solids: Quantum Theory of Molecules and Solids* vol 4 (New York: McGraw-Hill)
- [27] Cherepkov N A, Raseev G, Adachi J, Hikosaka Y, Ito K, Motoki S, Sano M, Soejima K and Yagishita A 2000 *J. Phys. B: At. Mol. Opt. Phys.* **33** 4213
- [28] Lucchese R R, Raseev G and McKoy V 1982 *Phys. Rev. A* **25** 2572
- [29] Choi H C, Rao R M, Mihill A G, Kakar S, Poliakoff E D, Wang K and McKoy V 1994 *Phys. Rev. Lett.* **72** 44
- [30] Adachi J, Kosugi N, Shigemasa E and Yagishita A 1996 *J. Phys. Chem.* **100** 19783
- [31] van der Straten P, Morgenstern R and Niehaus A 1988 *Z. Phys. D: At. Mol. Clusters* **8** 35
- [32] Carroll T X, Hahne J, Thomas T D, Berrah N, Bozek J and Kukk E 2000 *Phys. Rev. A* **61** 042503